Minimal State Non-Coherent Symbol MAP Detection of Continuous-Phase Modulations

Charles-Ugo Piat-Durozoi, *Student Member, IEEE*, Charly Poulliat, *Member, IEEE*, Nathalie Thomas, Marie-Laure Boucheret, Guy Lesthievent, and Emmanuel Bouisson

***Abstract*— Trellis-based detector is an effective method to demodulate non-coherent continuous-phase modulated sequences. Most of them have been derived for the maximum likelihood sequence estimation setting, while only few contributions have been proposed for the maximum *a posteriori* (MAP) symbol detection, required when soft information is needed for iterative detection and decoding. In this letter, we derive a new symbol MAP non-coherent receiver with reduced state space representation compared with the existing extended state-space-based approaches. While having the same performance, it enables a lower complexity.**

***Index Terms*— Trellis-based detector, non-coherent, continuous phase modulation, mutual information rate, spectral efficiency.**

I. Introduction

CPM is a particular modulation having a constant envelop waveform leading to excellent power efficiency [1], [9]. A second important aspect of CPM is the phase continuity yielding better spectral occupancy. The phase of a CPM signal for a given symbol depends on the cumulative phase of previous transmitted symbols known as the phase memory. Hence the decision taken on the current symbol must take into account the previous ones. Two types of CPM can be distinguished, partial response CPM which has a memory strictly greater than one symbol and full response CPM whose memory is exactly equal to one. Another important element of CPM is the modulation index which could restrain, in a particular case, the set of the phase memory to a finite set. In the non-coherent regime, two main approaches exist to demodulate/detect a sequence based on either block or trellis processing. Block detection can work for any value of modulation index and is robust to fast channel phase shifts when blocks are taken independently. Thus the channel coherence time must be at most of the order of the block size. Trellis based detection gives better performance than block detection for lower complexity but requires a constant phase shift over the whole trellis.

References [4] and [5] (respect. [6]) have implemented the receiver by block for a hard (respect. soft-decision) demodulation (originally applied for CPFSK only in [6]). The process can be summarized as follows. The block receiver does the correlation between the block of received symbols and all existing combinations of the same block length. The condition required to use this method is the absence of phase shift between symbols belonging to the same block since the phase continuity is exploited within the blocks. If we assume a ML block detection as in [4], the decision is made in the favor of the largest conditional probability. If a MAP detection is preferred [6], the demodulator computes the log-likelihood ratio (LLR) for each symbol/bit of the block based on the conditional and a priori probabilities.

TABLE I
Comparison With Main Existing Approaches

Reference paper	Algorithm/Criteria	State Space	Metrics	Complexity
[8]	$\neq$	$=$	$\neq$	$<$
[7]	$=$	$\neq$	$\neq$	$>$

[1] $=$ (respectively $\neq$) the reference paper has the same (respectively different) feature (”Criteria/State model/Metric”) than the proposed approach.
[2] $<$ (respectively $>$) the reference has a lower (respectively larger) complexity than the proposed approach.

A first trellis-based approach based on Viterbi algorithm had been presented in [8]. Thereafter [7] proposed a symbol MAP decoding algorithm similar to the well-known BCJR [3]. However the state cardinality proposed for the MAP detection in [7] is greater than the one presented in [8] for the ML detection. Indeed the author added to the state provided in [8] the accumulated phase given birth, in some ways, to an extended state space. The main differences between both approaches and the one proposed in this letter are summarized in Table I. We explicitly show in this letter that, by considering the state space given by [8], the direct derivation of the symbolwise non coherent MAP receiver for CPMs leads to the same bit error rate performance than the extended state space approach usually considered in the literature. An additional EXIT charts analysis shows that there is no information loss when considering the proposed reduced state space approach. This implies that [8] is effectively a sufficient state representation for non coherent detection, since no loss of information occurs. Moreover, the trellis resulting from state space [8] is minimal, in the sense that, for a given observation length, a non coherent trellis MAP detector having less states without performance loss cannot be found. This implies that this representation is the sole representation leading to minimal complexity for a given observation length.

The remainder of this letter is organized as follows. The next section provides a detailed exposition of the system model. Section III is devoted to the derivation of an exact mathe-

Manuscript received June 23, 2018; accepted July 10, 2018. Date of publication July 20, 2018; date of current version October 8, 2018. This work was supported by CNES and University of Toulouse (IRIT/Toulouse INP). The associate editor coordinating the review of this paper and approving it for publication was N. Zlatanov. *(Corresponding author: Charles-Ugo Piat-Durozoi.)*

C.-U. Piat-Durozoi is with IRIT/Toulouse INP, University of Toulouse, 31000 Toulouse, France, and also with TéSA, 31000 Toulouse, France (e-mail: charles-ugo.piat@tesa.prd.fr).

C. Poulliat, N. Thomas, and M.-L. Boucheret are with IRIT/Toulouse INP, University of Toulouse, 31000 Toulouse, France.

G. Lesthievent and E. Bouisson are with Systèmes de Télécommunications, CNES Toulouse, 31000 Toulouse, France.

Digital Object Identifier 10.1109/LCOMM.2018.2857773

matical formulation of the non-coherent trellis based receiver state space model. Thereafter the mutual information rate of the system is derived and subsequently used to compute the spectral efficiency (SE) in section IV. Section V gives some simulation results while Section VI concludes the letter.

II. System Model

At the transmitter, a binary message vector $\mathbf{b} = [b_0, \cdots, b_{K_b-1}] \in \mathbb{F}_2^{K_b}$ is mapped into a sequence $\mathbf{u} = [u_0, \ldots, u_{N_s-1}]$ belonging to the M-ary alphabet $\{0, \ldots, M-1\}$ (with M being a power of 2). Symbols are then modulated following the CPM modulation rule using Rimoldi's representation (see [2]). This can be seen as the serial concatenation of a continuous phase encoder (CPE) and a memoryless modulator. First, the CPE ensures the continuity between the transmitted continuous-time waveforms by accumulating the phase of each modulated symbol.

$$\phi_{k+1} = \phi_k + 2\pi h u_{k-L+1} \tag{1}$$

h is the modulation index ($h = \frac{P}{Q}$, with P and Q being relatively prime) and ϕ_k is the accumulated phase at the start of the k^{th} symbol. We note $\mathcal{Q}$ the set of Q values taken by the ϕ_k. L is a strictly positive integer referred to as the memory of the CPM. Then, the memoryless modulator maps the output of the CPE into a set X of M^L continuous-time waveforms. At the k^{th} symbol interval, the subset $u_{k-L+1}^k = \{u_{k-L+1}, \ldots, u_k\}$ matches $x_i(\tau)$ corresponding to the i^{th} signal of $X = \{x_i(\tau), i = 0 \ldots M^L - 1\}$ with [2], [6]

$$x_i(\tau) = \frac{A(\tau)}{\sqrt{T}} \cdot e^{j4\pi h \sum_{n=0}^{L-1} u_{k-n} q(\tau+nT)}, \quad \tau \in [0, T), \tag{2}$$

where $A(\tau)$ represents the Rimoldi representation's data independent terms and the index i is determined as follows

$$i = \sum_{n=0}^{L-1} u_{k-n} \cdot M^{L-1-n} \tag{3}$$

and

$$A(\tau) = e^{j\pi h(M-1)\left(\frac{\tau}{T} + (L-1) - 2\sum_{n=0}^{L-1} q(\tau+nT)\right)}. \tag{4}$$

In the expression above, T is the symbol period and the function $q(t)$ is the phase response that satisfies $q(t) = 0$ if $t \leq 0$, $q(t) = \frac{1}{2}$ if $t > LT$ and $q(t) = \int_0^t g(u)du$ if $0 < t \leq LT$. $g(u)$ is the frequency pulse depending on the kind of used CPM. The CPM complex baseband representation of the transmitted continuous-time waveform during the k^{th} symbol time of the observation interval is given by:

$$s_k(t) = \sqrt{Es} \cdot x_i(t) \cdot e^{j\phi_k} \tag{5}$$

The transmitted signal undergoes a phase rotation θ and is corrupted by an additive complex white Gaussian noise (AWGN), $n(t)$, with noise spectral density N_0. θ is assumed to be unknown and uniformly distributed on $[0, 2\pi]$. Es is the energy per symbol. The channel is said to be non-coherent. The corresponding complex-baseband received signal is given by, $\forall\, t \in [kT; (k+1)T)$,

$$r_k(t) = e^{j\theta} \cdot s_k(t) + n(t), \tag{6}$$

In this paper, perfect frequency and time synchronization are assumed. During the k^{th} symbol interval, the received signal $r_k(t)$ is passed through a bank of M^L matched filters whose impulse responses are given by $\bar{x}_i(-t)$, $i = 0, \ldots, M^L - 1$ where $\bar{x}_i(t)$ is the complex conjugate of $x_i(t)$. The sufficient statistics are the samples $r_{i,k}$ resulting from the correlation between $r_k(t)$ and $\bar{x}_i(-t)$. In the sequel, we adopt the following notation $\boldsymbol{r}_k = [r_{0,k}, \ldots, r_{M^L-1,k}]$ and the set of observations is given by $\boldsymbol{r}_0^{N_s-1} = [\boldsymbol{r}_0, \ldots, \boldsymbol{r}_{N_s-1}]$.

III. Non-Coherent MAP Trellis-Based Receiver

The non-coherent trellis-based receiver (TBR) is based on a trellis representation allowing us to use a modified version of the BCJR algorithm to compute the conditional probability of a symbol given the observations noted $p(u_k|\boldsymbol{r}_0^{N_s-1})$. Let $\delta_k = \{u_{k-N-L+2}, \ldots, u_{k-1}\}$ be a state of the trellis taking into account a series of $N + L - 2$ symbols $u_{k-N-L+2}^{k-1}$ (with $k \geq N + L - 2$). Based on this state space, we can differentiate the $L - 1$ symbols coming from the memory required by the partial response and the $N - 1$ additional symbols required when we extend the observation length in non-coherent regime to improve the performance. Those latter are called the correlated symbols in the sequel because they are used in the process of correlation between the observations and the existing combination of symbols. The reader will notice that the state cardinality of δ_k is reduced compared to [7]. Actually [7] included unnecessarily the accumulated phase ϕ to δ_k generating an extended state space. The transition between two states $\{\delta_k \rightarrow \delta_{k+1}\}$ corresponds to the transmitted symbol u_k. Based on this minimal state space model which can be shown optimal, we re-derive a modified version of the BCJR algorithm. At first, the conditional probability is developed as follows.

$$p(u_k|\boldsymbol{r}_0^{N_s-1}) \propto \sum_{\{\delta_k\}} \alpha_k(\delta_k)\beta_{k+1}(\delta_{k+1}) \cdot \gamma(\delta_k \rightarrow \delta_{k+1}, \boldsymbol{r}_{k-N+1}^k)p(u_k) \tag{7}$$

where

$$\begin{aligned}
&\gamma(\delta_k \rightarrow \delta_{k+1}, \boldsymbol{r}_{k-N+1}^k) \\
&\quad = p(\boldsymbol{r}_{k-N+1}^k|\delta_k, u_k), \alpha_k(\delta_k) \\
&\quad = p(\boldsymbol{r}_0^{k-N}|\boldsymbol{r}_{k-N+1}^{k-1}, \delta_k)p(\delta_k), \beta_{k+1}(\delta_{k+1}) \\
&\quad = p(\boldsymbol{r}_{k+1}^{N_s-1}|\boldsymbol{r}_{k-N+2}^k, \delta_{k+1}).
\end{aligned}$$

The forward-backward recursions can be calculated as

$$\begin{aligned}
\alpha_k(\delta_k) &= \sum_{\{\delta_{k-1}\}} \alpha_{k-1}(\delta_{k-1}) \cdot p(\boldsymbol{r}_{k-N}|\boldsymbol{r}_{k-N+1}^{k-1}, \delta_k, \delta_{k-1}) \\
&\quad \cdot p(u_{k-1}) \\
\beta_k(\delta_k) &= \sum_{\{\delta_{k+1}\}} \beta_{k+1}(\delta_{k+1}) \cdot p(\boldsymbol{r}_k|\boldsymbol{r}_{k-N+1}^{k-1}, \delta_k, \delta_{k+1}) \cdot p(u_k)
\end{aligned}$$

α_k and β_k read finally as follows

$$\begin{aligned}
\alpha_k(\delta_k) &= \sum_{\{\delta_{k-1}\}} \alpha_{k-1}(\delta_{k-1}) \frac{\gamma(\delta_{k-1} \rightarrow \delta_k, \boldsymbol{r}_{k-N}^{k-1})}{p(\boldsymbol{r}_{k-N+1}^{k-1}|u_{k-1}, \delta_{k-1})} p(u_{k-1}) \\
\beta_k(\delta_k) &= \sum_{\{\delta_{k+1}\}} \beta_{k+1}(\delta_{k+1}) \frac{\gamma(\delta_k \rightarrow \delta_{k+1}, \boldsymbol{r}_{k-N+1}^k)}{p(\boldsymbol{r}_{k-N+1}^{k-1}|u_k, \delta_k)} p(u_k)
\end{aligned} \tag{8}$$

The branch metric can be computed as

$$\gamma(\delta_k \rightarrow \delta_{k+1}, \boldsymbol{r}_{k-N+1}^{k}) = p(\boldsymbol{r}_{k-N+1}^{k}|\delta_k, u_k) \propto I_0\left(\rho \cdot |\mu(u_{k-N-L+2}^{k})|\right) \quad (9)$$

where $\rho = 2\sqrt{Es}/N_0$ and I_0 the modified zero order Bessel function of the first kind,

$$\mu(u_{k-N-L+2}^{k}) = \sum_{i=k-N+1}^{k} r_{u_{i-L+1}^{i},i} \cdot e^{-j2\pi h \sum_{n=k-N-L+2}^{i-L} u_n}$$

which finally gives the following recursions

$$\alpha_k(\delta_k) \propto \sum_{\{\delta_{k-1}\}} \alpha_{k-1}(\delta_{k-1}) \frac{I_0\left(\rho \cdot |\mu(u_{k-N-L+1}^{k-1})|\right)}{I_0\left(\rho \cdot |\mu(u_{k-N-L+2}^{k-1})|\right)} p(u_{k-1})$$

$$\beta_k(\delta_k) \propto \sum_{\{\delta_{k+1}\}} \beta_{k+1}(\delta_{k+1}) \frac{I_0\left(\rho \cdot |\mu(u_{k-N-L+2}^{k})|\right)}{I_0\left(\rho \cdot |\mu(u_{k-N-L+2}^{k-1})|\right)} p(u_k) \quad (10)$$

N.B. $I_0(\rho \cdot |\mu(u_{k-N-L+2}^{k-1})|)$ is seen as a normalization factor which is not taken into account in [8] when ML criterion is applied. We note δ'_k the extended state space described in [7]. Metrics associated to δ_k can be derived from the metrics associated to δ'_k by averaging over the accumulated phase.

$$\begin{aligned} \gamma(\delta_k \rightarrow \delta_{k+1}, \boldsymbol{r}_{k-N+1}^{k}) &= \frac{1}{Q} \cdot \sum_{\{\phi_{k-N+1}\}} \gamma(\delta'_k \rightarrow \delta'_{k+1}, \boldsymbol{r}_{k-N+1}^{k}) \\ \alpha_k(\delta_k) &= \sum_{\{\phi_{k-N+1}\}} \alpha(\delta'_k) \\ \beta_k(\delta_k) &= \frac{1}{Q} \cdot \sum_{\{\phi_{k-N+1}\}} \beta_k(\delta'_k) \end{aligned} \quad (11)$$

The complexity of the proposed algorithm, evaluated in terms of number of real operations, is of the order of $\mathcal{O}(8NM^{N+L-1})$. Being the MAP extension of [8] that considers a Viterbi decoding approach, we roughly have twice the complexity of the latter approach, that can be seen as a forward only version. Note that we address the symbolwise MAP decoding for enabling soft iterative non coherent detection of CPMs signal, which cannot be done using a Viterbi based detection. Finally, our approach has a lower complexity than [7] evaluated as $\mathcal{O}(8(N+Q)M^{N+L-1})$.

IV. Asymptotic Performance Analysis

The mutual information rate of finite-state channels have been studied in [10] and [11]. The mutual information rate between the channel input source $\mathcal{U}$ and the channel output $\mathcal{R}$ can be described as follows [12] :

$$I(\mathcal{U}, \mathcal{R}) = \lim_{N_s \rightarrow \infty} \frac{1}{N_s} I(u_0^{N_s-1}, \boldsymbol{r}_0^{N_s-1}|\delta_{N+L-2}) \quad (12)$$

We denote by $I(u_0^{N_s-1}, \boldsymbol{r}_0^{N_s-1}|\delta_{N+L-2})$ the mutual information between the input process $u_0^{N_s-1}$ and the output process $\boldsymbol{r}_0^{N_s-1}$ conditioned by the initial state δ_{N+L-2}. Its general expression is the following [13]

$$\begin{aligned} &I(u_0^{N_s-1}, \boldsymbol{r}_0^{N_s-1}|\delta_{N+L-2}) \\ &\quad = (N_s - (N+L-2))\, log_2(M) \\ &\qquad + E\left[\sum_{k=N+L-2}^{N_s-1} log_2\left(p(u_k|\delta_{N+L-2}^{k}, \boldsymbol{r}_0^{N_s-1})\right)\right] \end{aligned} \quad (13)$$

Computation of $p(u_k|\delta_{N+L-2}^{k}, \boldsymbol{r}_0^{N_s-1})$ in equation (13) can be found in [14]. The idea is to compute the probability of a symbol knowing perfectly all the previous states from the beginning of the transmission. This is equivalent to perform the BCJR algorithm as usual but taking into account the complete knowledge of the forward recursion i.e α is fixed to 1 for the correct state and 0 to all other states. γ and β remained unchanged beside the traditional BCJR. Then dividing by the source length N_s gives the result.

Asymptotic analysis can also be carried out using EXIT charts. Reference [16] pointed out that the achievable rate is approximately equal to the area under the EXIT curve for a given operating point (proven over the erasure channel [15]). In other words, the experimental achievable rate noted $\mathcal{R}^*$ is linked with I_e, the mutual information at the output of decoder: $\mathcal{R}^* \simeq \int_0^1 I_e(x)\mathrm{d}x$. Readers unfamiliar to EXIT chart could refer to Hagenauer's introduction on EXIT chart in [16]. To effectively compare various CPM, it is necessary to compute the achievable information rate under a bandwidth constraint. 1 Hz of available bandwidth is usually taken. Thus we define the normalized bandwidth as $\mathcal{B}_n = log_2(M)/(\mathcal{B}_{99} \cdot T)$. T is taken equal to 1 (since only 1 Hz bandwidth is available) and $\mathcal{B}_{99}$ is given as the bandwidth that contains 99% of the power of the uncoded complex baseband signal. Then the spectral efficiency is obtained by multiplying the achievable information rate by the normalized bandwidth. Fig. 1 shows the spectral efficiency of a binary GMSK with $\mathcal{B}_n \sim 0.88$.

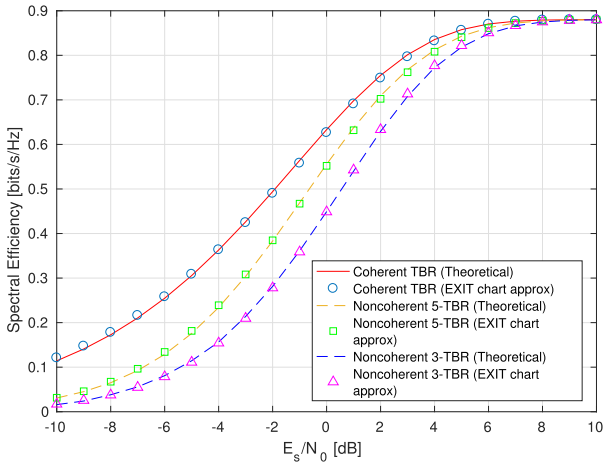

Fig. 1. SE of binary GMSK with $h = 1/2$, $L = 2$ $BT = 0.25$.

V. Simulation Results

Fig. 2 shows binary GMSK and quaternary 2RC EXIT charts for an operating point of $E_s/N_0 = 0$ dB. Curves have been drawn in non-coherent regime based on: (a) the extended

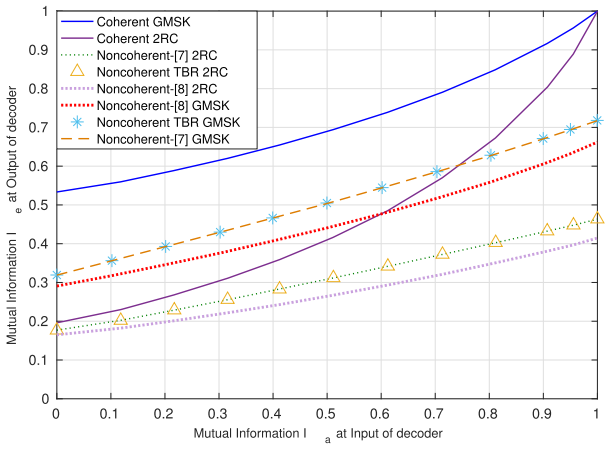

Fig. 2. Exit charts of binary GMSK $h = 1/2$, $L = 2$ and $BT = 0.25$ and quaternary 2RC with $h = 1/4$ ($N = 3$ for both).

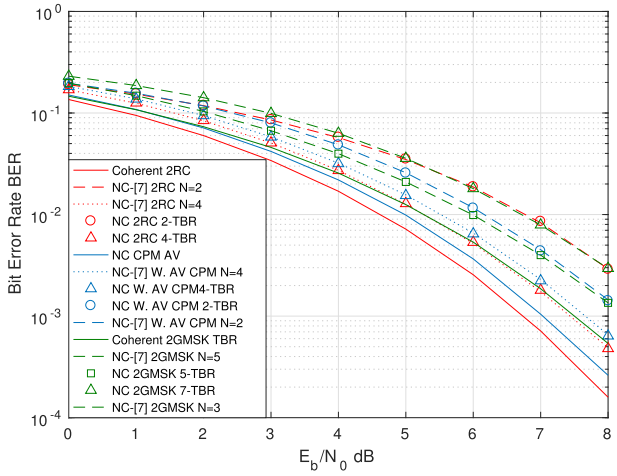

Fig. 3. BER: 2GMSK with $h = 1/2, M = 2, BT = 0.25$, Weigthed AV CPM [17] $h = 1/3, M = 4$, 2RC $h = 1/3, M = 4$.

state space from [7] noted noncoherent- [7] (NC- [7] Fig. 3), (b) the optimal state space model based on the ML metric presented in [8] noted noncoherent- [8] and (c) the non-coherent TBR state space proposed in section III. Exit charts graph brings to light two major aspects of this paper. First the receiver proposed in [7] and the non-coherent TBR are superimposed meaning the two models are equivalent from both spectral efficiency and performance perspective (see also Fig. 3). Yet the state space reduction permits to reach the minimal state space required for an optimal detection for a given complexity (ie. the number of correlated symbols). Thus the model propose in [7] may be reduced for equal performance (i.e the number of state can be reduced from $Q \cdot M^{N+L-2}$ to M^{N+L-2}). Secondly, the ML metric ([8]) differs by the absence of the normalization part when compared with the MAP presented in this paper in (10). Both metrics have similar performance exclusively for zero a priori ($I_a = 0$). When the a priori information increases the non-coherent TBR outperforms [8]. It means iterative decoding will be more efficient with the non-coherent TBR metric than with the one provided in [8]. The spectral efficiency (based on (13)/EXIT chart) and the bit error rate (BER) have been plotted in Fig. 1 and 3 for several types of CPM widely used in satellite and aeronautical communications [17]. It brings to light two important aspects: there is no information to gain from the state space expansion and the performance is improved when N increases. Thus state δ_k is sufficient but also minimal since for a given observation length N, you cannot find a non coherent trellis MAP detector having less states without performance loss. Simulation relative to the impact of residual frequency synchronization error have also been carried out. For instance for a 2GMSK ($N = 2, h = 1/2, M = 2$, $BT = 0.25$), a frequency shift of $T\Delta f = 2\%$ (respect. 3%) the symbol rate generates 0.5dB (respect. 1dB) loss for a BER equal to 10^{-5}.

VI. Conclusion

In this paper, a trellis based MAP detector with a minimal and sufficient state space for CPM suited for non-coherent communications is proposed. This latter has a lower complexity than the extended state space approach usually considered in the literature [7] without performance penalties.

References

[1] J. G. Proakis, *Digital Communications*, 4th ed. New York, NY, USA: McGraw-Hill, 2001.
[2] B. E. Rimoldi, "A decomposition approach to CPM," *IEEE Trans. Inf. Theory*, vol. IT-34, no. 2, pp. 260–270, Mar. 1988.
[3] L. Bahl, J. Cocke, F. Jelinek, and J. Raviv, "Optimal decoding of linear codes for minimizing symbol error rate," *IEEE Trans. Inf. Theory*, vol. IT-20, no. 2, pp. 284–287, Mar. 1974.
[4] M. K. Simon and D. Divsalar, "Maximum-likelihood block detection of noncoherent continuous phase modulation," *IEEE Trans. Commun.*, vol. 41, no. 1, pp. 90–98, Jan. 1993.
[5] D. Divsalar and M. K. Simon, "Multiple-symbol differential detection of MPSK," *IEEE Trans. Commun.*, vol. 38, no. 3, pp. 300–308, Mar. 1990.
[6] M. C. Valenti, S. Cheng, and D. Torrieri, "Iterative multisymbol noncoherent reception of coded CPFSK," *IEEE Trans. Commun.*, vol. 58, no. 7, pp. 2046–2054, Jul. 2010.
[7] G. Colavolpe, G. Ferrari, and R. Raheli, "Noncoherent iterative (turbo) decoding," *IEEE Trans. Commun.*, vol. 48, no. 9, pp. 1488–1498, Sep. 2000.
[8] D. Raphaeli and D. Divsalar, "Multiple-symbol noncoherent decoding of uncoded and convolutionally coded continuous phase modulation," *J. Commun. Netw.*, vol. 1, no. 4, pp. 238–248, Dec. 1999.
[9] J. B. Anderson *et al.*, *Digital Phase Modulation*. New York, NY, USA: Plenum, 1986.
[10] D. M. Arnold, H.-A. Loeliger, P. O. Vontobel, A. Kavcic, and W. Zeng, "Simulation-based computation of information rates for channels with memory," *IEEE Trans. Inf. Theory*, vol. 52, no. 8, pp. 3498–3508, Aug. 2006.
[11] S. Yang, "The capacity of communication channels with memory," Ph.D. dissertation, Division Eng. Appl. Sci., Harvard Univ., Cambridge, MA, USA, 2004.
[12] S. Yang, A. Kavčić, and S. Tatikonda, "Feedback capacity of finite-state machine channels," *IEEE Trans. Inf. Theory*, vol. 51, no. 3, pp. 799–810, Mar. 2005.
[13] T. M. Cover and J. A. Thomas, *Elements of Information Theory*. New York, NY, USA: Wiley, 1991.
[14] K. Padmanabhan, S. Ranganathan, S. P. Sundaravaradhan, and O. M. Collins, "General CPM and its capacity," in *Proc. IEEE ISIT*, Adelaide, SA, Australia, Sep. 2005, pp. 750–754.
[15] A. Ashikhmin, G. Kramer, and S. ten Brink, "Extrinsic information transfer functions: Model and erasure channel properties," *IEEE Trans. Inf. Theory*, vol. 50, no. 11, pp. 2657–2673, Nov. 2004.
[16] J. Hagenauer, "The exit chart—Introduction to extrinsic information transfer in iterative processing," in *Proc. EUSIPCO*, Vienna, Austria, 2004, pp. 1541–1548.
[17] *Digital Video Broadcasting (DVB); Second Generation DVB Interactive Satellite System (DVB-RCS2); Part 1: Overview and System Level Specification*, document ETSI EN 301 545-2 V1.1.1, 2013.